





Physical properties of MnSi at extreme doping with Co: Quantum criticality

A. E. Petrova , S. Yu. Gavrillkin, and A. Yu. Tsvetkov
P. N. Lebedev Physical Institute, Leninsky Prospekt, 53, 119991 Moscow, Russia

Dirk Menzel  and Julius Grefe
Institut für Physik der Kondensierten Materie, Technische Universität Braunschweig, D-38106 Braunschweig, Germany

S. Khasanov 
Institute for Solid State Physics of RAS, 142432 Chernogolovka, Russia

S. M. Stishov *
P. N. Lebedev Physical Institute, Leninsky Prospekt, 53, 119991 Moscow, Russia

 (Received 15 April 2022; revised 9 June 2022; accepted 30 June 2022; published 11 July 2022)

Samples of $(\text{Mn}_{1-x}\text{Co}_x)\text{Si}$ with $x = 0.15$ and $x = 0.17$ were grown, and their physical properties: magnetization, magnetic susceptibility, resistivity, and heat capacity were studied. The data analysis included previous results at $x = 0.057, 0.063$, and 0.09 . The doping of MnSi with Co completely destroys the helical phase transition, but it saves the helical fluctuation area normally situated slightly above the phase-transition temperature. This area, spreading from ~ 5 to 0 K does not change much with doping and forms some sort of helical fluctuation cloud, revealing the quantum critical properties: $C_p/T \rightarrow \infty$ at $T \rightarrow 0$.

DOI: [10.1103/PhysRevB.106.014406](https://doi.org/10.1103/PhysRevB.106.014406)

I. INTRODUCTION

MnSi is an itinerant magnet with the Dzyaloshinskii-Moriya interaction, which has a phase transition to the spin helical phase at ~ 29 K. Applying pressure to the sample of MnSi leads to the decrease in transition temperature and finally to the disappearance of the spin ordered phase at ~ 14 kbars and near-zero temperature. This particular point (0 K, 14 kbar) in the phase diagram of MnSi can be a quantum critical point or just a quantum phase transition [1–3]. In an attempt to resolve this question, a number of doping experiments with MnSi were performed.

The study of quantum criticality in the model substance of MnSi by doping with Fe and Co were described in Refs. [4–7]. The main idea was to imitate the high-pressure condition by substituting Mn with smaller ions [5–7] that would place the material in a situation where the pure MnSi experiences a quantum phase transition at zero temperature. Of course, the substitution would cause some structural disorder and influence the electron structure of materials that should be taken into account in an analysis of experimental data. As was shown in Refs. [4–6] the helical phase transition in $(\text{Mn}_{1-x}\text{Fe}_x)\text{Si}$ can be seen close to zero temperature at a doping level of $x \approx 0.16$ – 0.19 . At the same time, neutron scattering studies [8–10] unambiguously show that the loss of chiral spin ordering in $(\text{Mn}_{1-x}\text{Fe}_x)\text{Si}$ with increasing Fe concentration occurs in two steps. The first one corresponds to the disappearance of long-range spin correlation resulting in

the phase transition from the helimagnetic to the paramagnetic state ($x \sim 0.11$). The second step consists of losing short-range chiral spin order ($x \sim 0.17$), which can be seen in the destruction of the helical fluctuation maxima observed, for instance, in the heat-capacity data for pure MnSi, $(\text{Mn}_{1-x}\text{Fe}_x)\text{Si}$, and $(\text{Mn}_{1-x}\text{Co}_x)\text{Si}$ [5–7]. Although a trace of the chiral structure can be identified even at $x \sim 0.20$ (Ref. [10]).

For $(\text{Mn}_{1-x}\text{Co}_x)\text{Si}$, doping MnSi with Co completely destroys the phase transition at $x \approx 0.04$ and about 8 K. However, the helical fluctuation maxima or humps, which are normally situated slightly above the phase-transition temperature, survive even much heavier doping [7]. The temperatures of the maxima appears not to be very sensitive to doping above $x \approx 0.05$. This intriguing feature led to a tentative conclusion, which should be verified, that at large concentration of Co impurity a cloud of the helical fluctuations arises close to 0 K (Ref. [7]). With all that in mind, we decided to extend our previous study [7] by including samples with larger concentrations of Co dopant that probably could shed a new light on this problem.

II. EXPERIMENTAL

The samples of $(\text{Mn}_{1-x}\text{Co}_x)\text{Si}$ with $x > 0.05$ were prepared by a procedure, described in Ref. [7], and two of them with $x = 0.15$ and $x = 0.17$ as determined by the electron probe microanalysis were selected for further examination. The lattice parameters of the samples, measured by the x-ray powder diffraction, are correspondingly 4.5464 and 4.5457 Å. Magnetic, heat-capacity, and resistivity measurements were performed to characterize the (Mn,Co)Si samples.

*stishovsm@lebedev.ru

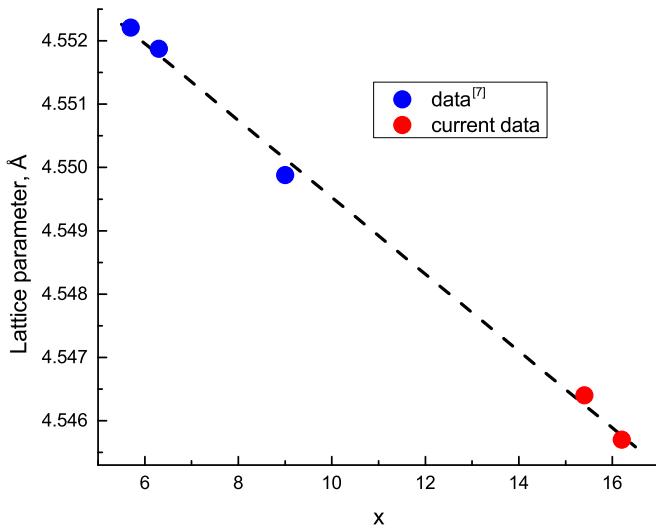


FIG. 1. The lattice parameters of $(\text{Mn}_{1-x}\text{Co}_x)\text{Si}$ as a function of Co content. The observed linear dependence (Vegard rule) indicates that the Co component forms a solid solution with MnSi at the given concentrations.

All measurements were made making use the Quantum Design physical property measurement system system with the heat capacity and vibrating magnetometer moduli and the He-3 refrigerator. The resistivity was measured with the standard four terminals scheme using the spark welded Pt wires as electrical contacts.

The experimental data are shown in Figs. 1–3, 5, 8, and 9.

III. RESULTS AND DISCUSSION

Figure 1 illustrates a dependence of the lattice parameters of $(\text{Mn}_{1-x}\text{Co}_x)\text{Si}$ on the Co content. Note that the lattice parameter of the material with $x \approx 0.15$ – 0.17 reaches the

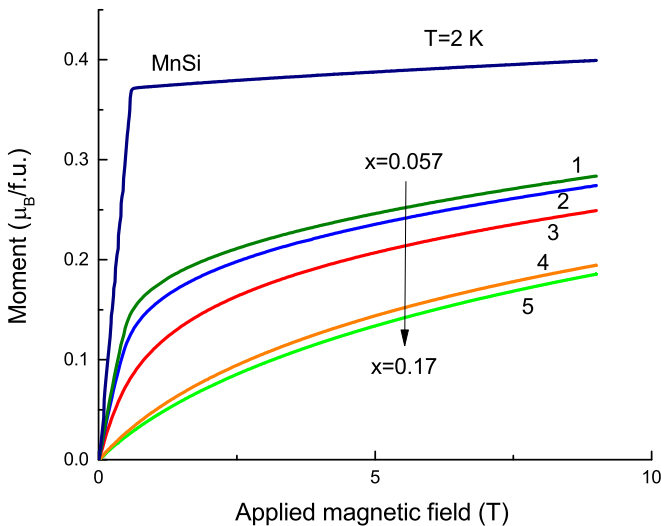


FIG. 2. Magnetization curves for $(\text{Mn}_{1-x}\text{Co}_x)\text{Si}$ in comparison with one for pure MnSi. (1–5: $x = 0.17, 0.15, 0.09, 0.063,$ and 0.057).

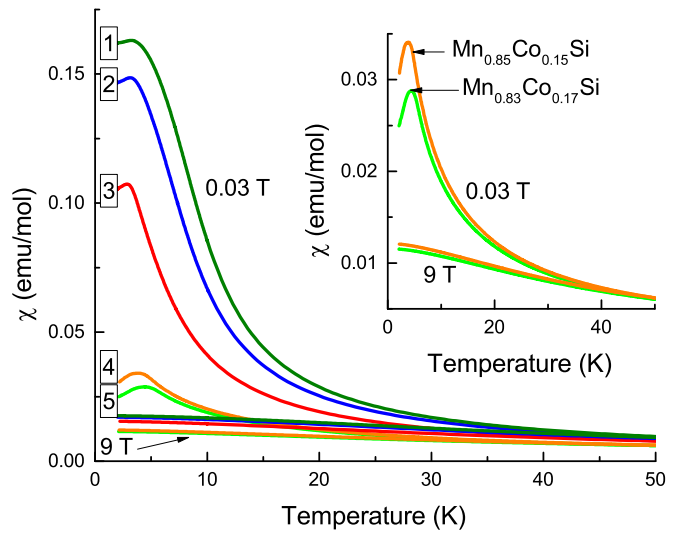


FIG. 3. Magnetic susceptibility of $(\text{Mn}_{1-x}\text{Co}_x)\text{Si}$ as a function of temperature at $0.03T$ and $9T$. See an enlarged plot of new data in the inset. (1–5: $x = 0.17, 0.15, 0.09, 0.063,$ and 0.057).

corresponding value for pure MnSi at the quantum phase-transition phase point at pressure about 14 kbars [6].

The magnetization curves of $(\text{Mn}_{1-x}\text{Co}_x)\text{Si}$, including those studied earlier [7] are shown in Fig. 2. The curves are naturally shifted with the Co concentration changing a form and gradually losing features of saturation. That was observed also in Ref. [5] at smaller Co concentrations.

In fact, as seen in Fig. 2, a saturation of magnetization does not occur in the doped samples even at magnetic fields to 9 T. It should be noted that a spin system in heavily doped $(\text{Mn}_{1-x}\text{Co}_x)\text{Si}$ samples at low temperatures has a kind of disordered structure complicated by the intense helical fluctuations [11,12] and spins of the Co impurity. Why all this prevents the magnetization from saturation remains to be seen.

Nevertheless, as one can see in Fig. 3, there is clear evidence of a peculiar behavior of magnetic susceptibility (maxima) that is most certainly intrinsically connected with

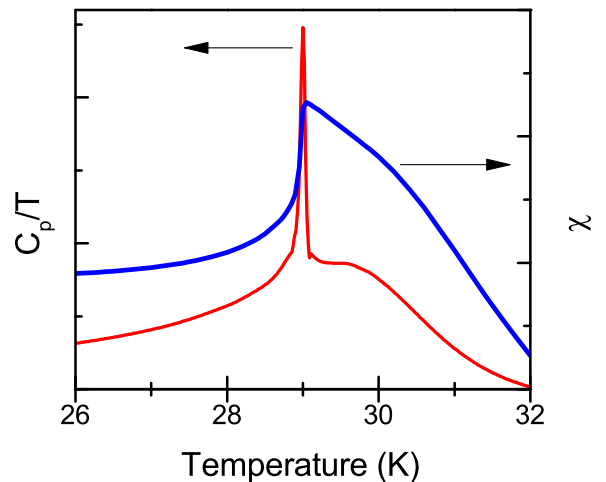


FIG. 4. Schematic of magnetic susceptibility and heat capacity at the phase transition in pure MnSi after Ref. [13].

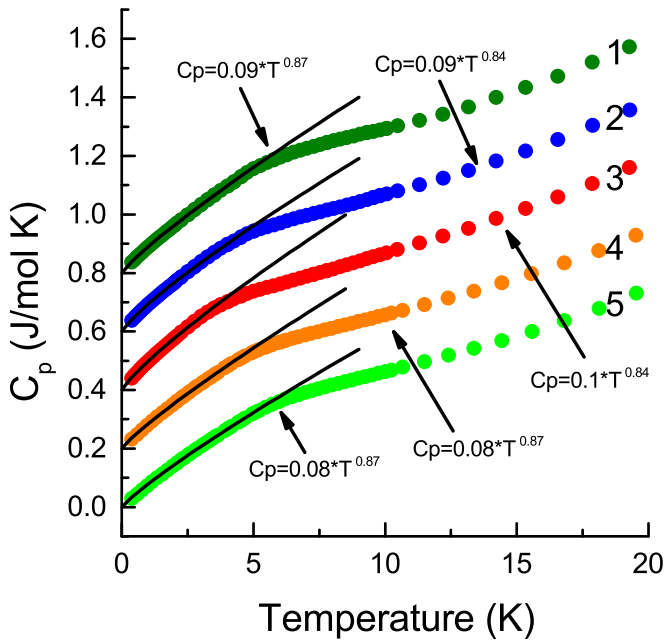


FIG. 5. Heat capacity of $(\text{Mn}_{1-x}\text{Co}_x)\text{Si}$. Fitting of the low-temperature part of heat capacity to the power function is illustrated. The values of the power exponents shown in the plot. The total error of shown exponents can be estimated as ± 0.02 . The data are shown with offsets for better viewing. (1–5: $x = 0.057, 0.063, 0.09, 0.15,$ and 0.17).

the inflection point on $\chi(T)$ curve of pure MnSi slightly above the phase transition point [13]. In turn, the inflection point in MnSi corresponds to the helical fluctuation maximum discovered in heat-capacity measurements in the same range of temperature as it depicted in Fig. 4, which is a schematic of magnetic susceptibility and heat-capacity behavior at the phase transition in pure MnSi [13]. A fluctuation nature of the observed maximum in MnSi is evident from small-angle neutron studies [11,12,14]. Monte Carlo calculations of the classical spin system with the chiral interaction support this conclusion [15]. There is no reason to think that the corresponding maxima in the doped systems have a different nature. So, it suggests that the helical fluctuations survive the heavy doping of MnSi with Co.

Support for that follows from the heat-capacity measurements shown in Fig. 5, where the new results are displayed together with existing data [7]. As is seen in Fig. 5 the heat-capacity curves noticeably change their slopes at temperatures about 5 K. The low-temperature parts of the curves can be described by a power function with exponents less than 1 (Fig. 5). This immediately leads to the diverging ratio C_p/T , which is a signature of quantum critical behavior as shown in Fig. 6. The slope change in the heat-capacity curves (Fig. 5) becomes more evident after a subtraction from the heat-capacity curve at zero magnetic field the corresponding curve at 9 T as was suggested in Ref. [7] (see Fig. 7). Application of strong magnetic fields to magnetic materials suppress spin fluctuations and, hence, corresponding contributions to heat capacity. In result only phonon and electron excitations are left in the magnetized material and the referred above subtraction leaves the spin-fluctuation part intact. But as is seen in Fig. 2

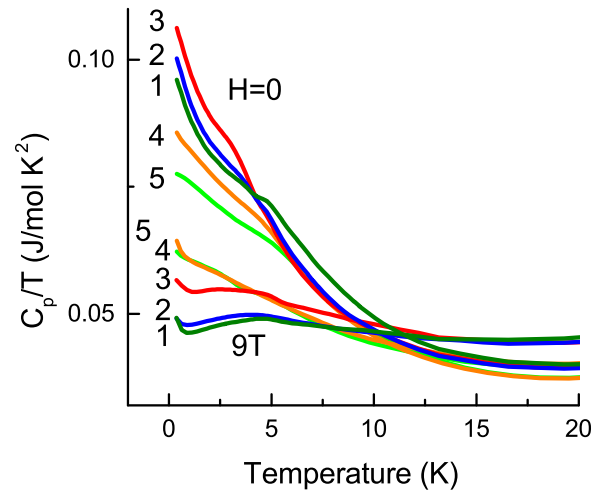


FIG. 6. The ratio C_p/T for $(\text{Mn}_{1-x}\text{Co}_x)\text{Si}$ samples as a function of temperature at zero and 9 T magnetic fields. It is seen that diverging of C_p/T is suppressed by strong magnetic field for samples studied earlier [7], but this is probably not a case for two new samples with the increased concentration of Co. (1–5: $x = 0.17, 0.15, 0.09, 0.063,$ and 0.057).

a magnetic field of 9 T does not suppress completely the spin fluctuations in $(\text{Mn}_{1-x}\text{Co}_x)\text{Si}$ with $x = 0.15$ and 0.17 . That is probably why new curves look somewhat different.

Behavior of C_p/T of all samples $(\text{Mn}_{1-x}\text{Co}_x)\text{Si}$ is shown in Fig. 6. The diverging of C_p/T at $T \rightarrow 0$ K is obvious, but a weaker response of samples with $x = 0.15$ and $x = 0.17$

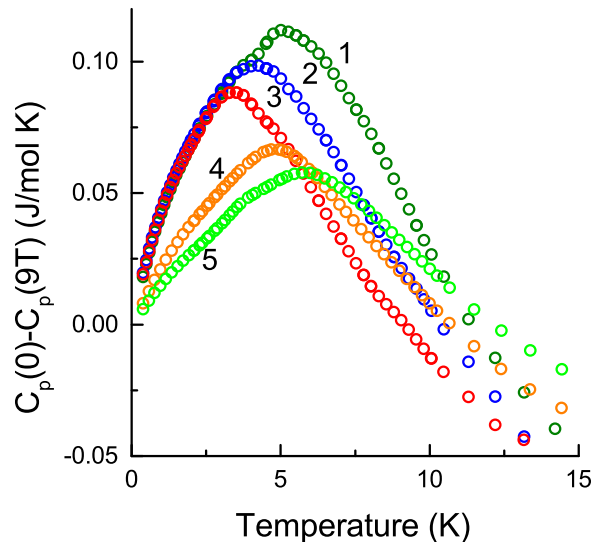


FIG. 7. The difference between heat capacity at zero magnetic field $C_p(0)$ and heat capacity at 9 T $C_p(9T)$ for $(\text{Mn}_{1-x}\text{Co}_x)\text{Si}$ samples. This manipulation implies a subtraction of some background contributions, including phonon and electron ones to the heat capacity leaving the spin fluctuation part intact. But as is seen in Fig. 2 a magnetic field of 9 T does not suppress completely the spin fluctuations in $(\text{Mn}_{1-x}\text{Co}_x)\text{Si}$ with $x = 0.15$ and 0.17 . That is probably why new curves look somewhat different. (1–5: $x = 0.17, 0.15, 0.09, 0.063,$ and 0.057).

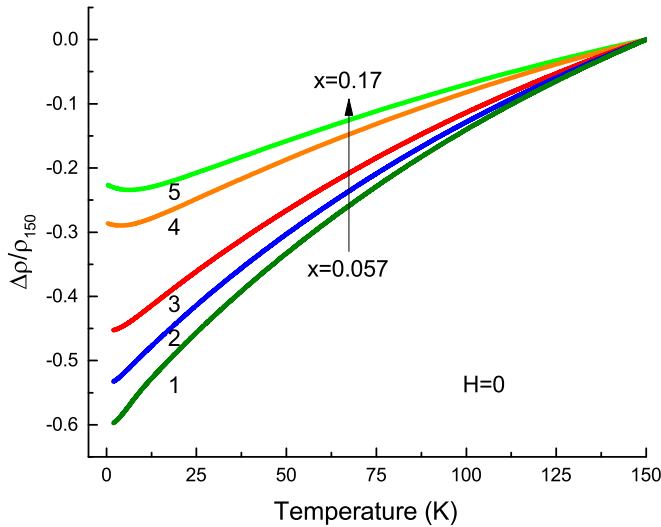


FIG. 8. Dependence of resistivity of $(\text{Mn}_{1-x}\text{Co}_x)\text{Si}$ on temperature. Data are modified accordingly to the formula $\Delta R/R_{150\text{K}}$ for better comparison. (1–5: $x = 0.17, 0.15, 0.09, 0.063,$ and 0.057).

to magnetic fields corresponds to their decreased magnetic susceptibility (see Fig. 3).

The resistivity measurements are illustrated in Figs. 8–10. As seen in Fig. 8, the expected temperature dependence of resistivity becomes smaller with the increased doping. But the weak localization features, which are upturns of the resistivity curves at low temperatures in samples with $x = 0.15$ and $x = 0.17$ (see Fig. 9), were not anticipated based on the heat-capacity data showing no distinct differences between the samples. So, the conductivity electrons probably do not contribute to the magnetic fluctuation phenomena.

Temperature derivatives of resistivity $(\text{Mn}_{1-x}\text{Co}_x)\text{Si}$, depicted in Fig. 10, show progressive degradation of the specific features (maxima of corresponding curves) with doping, therefore, likely indicating that the electron scattering on magnetic fluctuations becomes dominated by the impurity scattering. In this connection we have to remember that the temperature derivative of resistivity in a case of strong spin fluctuations demonstrates a sharp maximum [13].

We can see in Fig. 11 that the helical fluctuations do not disappear with heavy doping of Co. Moreover, the temperatures of fluctuation maxima are practically not changed with Co concentration, in contrast to the behavior of the phase-transition temperature. So, we have to confirm our former conclusion that, at large concentrations of Co impurity, a cloud of the helical fluctuations spreading over a significant range of concentrations and temperatures arises in the region of 0–5 K (Ref. [7]). Some insight can be obtained from Fig. 12 where a result of the Monte Carlo modeling of behavior of a classical spin system with the frozen impurities in interstitial positions is reproduced from Ref. [16]. As is seen, the helical phase transition in this spin system disappears with doping, whereas the fluctuation maximum is not changed at all. Probably just the frozen nature of impurities and not their exact positions are responsible for such a behavior of fluctuations.

It needs to be recalled that as a difference with the spin model, our real $(\text{Mn}_{1-x}\text{Co}_x)\text{Si}$ systems experience a regular

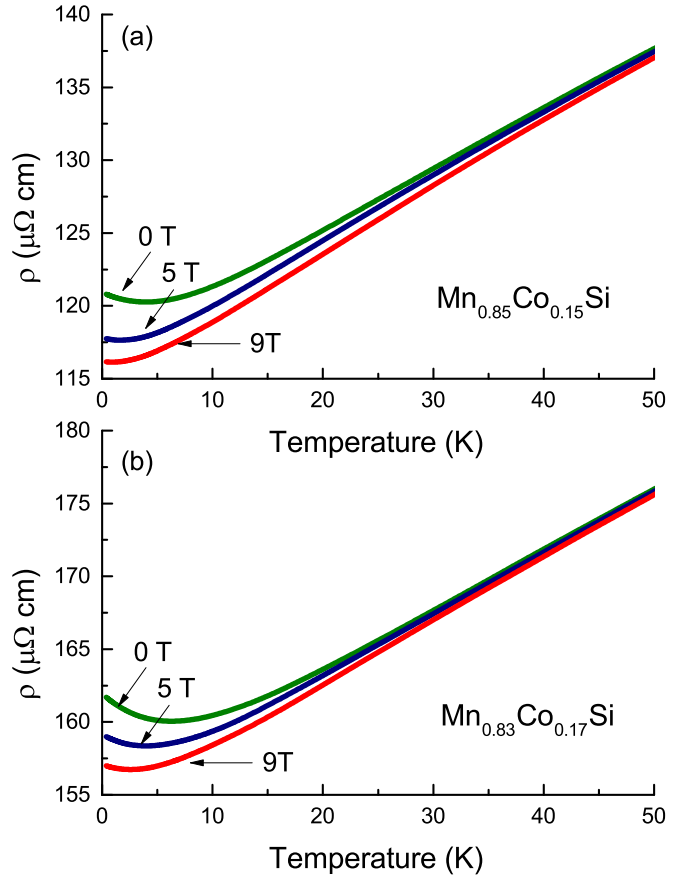


FIG. 9. Dependence of resistivity of $(\text{Mn}_{1-x}\text{Co}_x)\text{Si}$ on temperature at various magnetic fields. The features of weak localization (upturn of the resistivity curves), which partly suppressed by the magnetic field, are evident at low temperature.

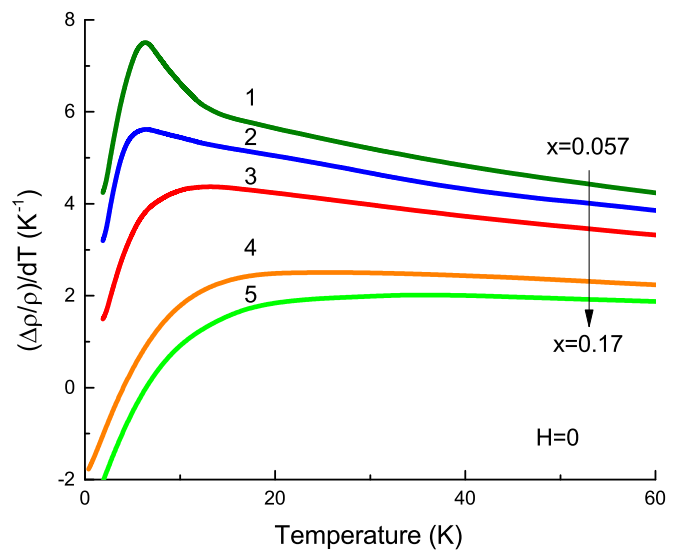


FIG. 10. Temperature derivatives of resistivity of the samples $(\text{Mn}_{1-x}\text{Co}_x)\text{Si}$. Note negative values of the derivatives for $x = 0.15$ and $x = 0.17$ at low temperatures. (1–5: $x = 0.17, 0.15, 0.09, 0.063,$ and 0.057).

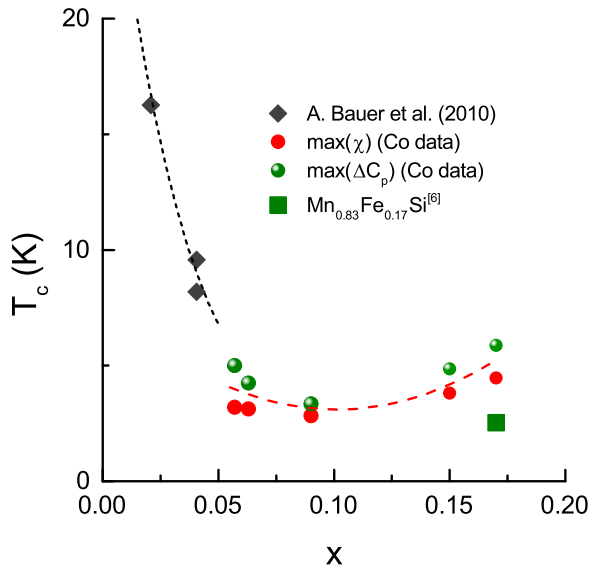


FIG. 11. Temperature of fluctuation maxima as a function of Co concentration. Phase-transition temperature occurring at low Co content is also shown as black squares [5]. In Ref. [5] phase-transition temperatures were determined from the temperature dependence of magnetic moments. Current fluctuation maxima data were taken as the χ maxima (Fig. 3) and maxima of ΔC_p (Fig. 7). Note that the Fe square data point corresponds to the sample studied in Ref. [6]. Corrected composition was used. Coordinates of the data points with $x = 0.15$ and $x = 0.17$ calculated from the heat capacity obviously influenced by the problem pointed out in the caption of Fig. 7.

volume decrease on doping (see Fig. 1) that is equivalent to hydrostatic compression of the material. So, if we try to describe our finding (Fig. 11) in terms of temperature and pressure it would look, such as the diagram depicted in Fig. 13. The suggested extended region of helical fluctuations in Fig. 13 probably correlates with early findings of the non-Fermi-liquid behavior [17] and the partial order [18] in pure MnSi at pressures above the magnetic-phase transition and at low temperature.

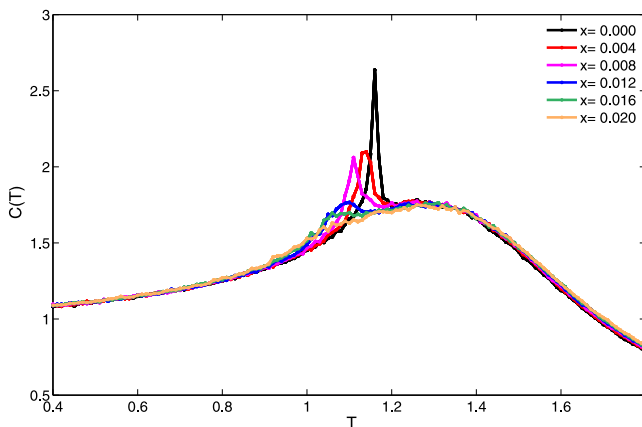


FIG. 12. Monte Carlo modeling the heat-capacity behavior of a classical spin system with impurities situated in interstitial positions for different doping concentrations. Reproduced from Ref. [16].

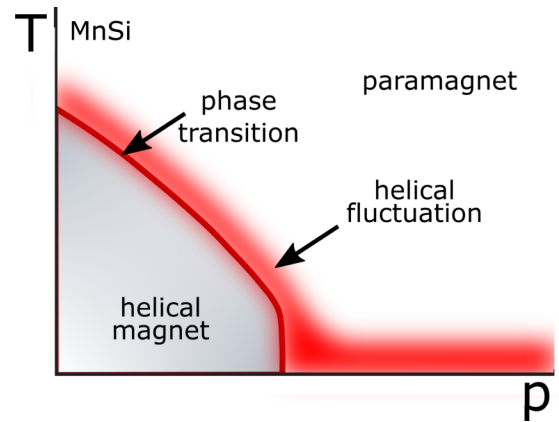


FIG. 13. Tentative T - P phase diagram for an itinerant magnet with the Dzyaloshinskii-Moriya interaction.

IV. SUMMARY AND CONCLUSION

(1) The observed linear dependence of the lattice parameters of $(\text{Mn}_{1-x}\text{Co}_x)\text{Si}$ (Vegard rule) indicates that the Co doping component forms a solid solution with MnSi at the studied concentrations (Fig. 1).

(2) A saturation of magnetization does not occur in the doped samples to 9 T (Fig. 2). This correlates with a weak response of the diverging part of C_p/T to a strong magnetic field.

(3) The helical fluctuations survive the heavy doping of MnSi with Co (Fig. 3).

(4) The low-temperature parts of the heat-capacity curves can be described by a power function with exponents less than 1e. This immediately leads to the diverging ratio C_p/T , which is a signature of quantum critical behavior (Fig. 5).

(5) The weak localization features for samples with $x = 0.15$ and $x = 0.17$ (see Fig. 9) were observed.

(6) Temperature derivatives of resistivity of $(\text{Mn}_{1-x}\text{Co}_x)\text{Si}$ show progressive degradation of the specific features of corresponding curves with doping, probably indicating that electron scattering on magnetic fluctuations becomes dominated by the impurity scattering (Fig. 10).

(7) Helical fluctuations do not disappear with heavy doping by Co. Moreover, the temperatures of fluctuation maxima practically are not changed with Co concentration, as a contrast to a behavior of the phase-transition temperatures (Fig. 11). So a cloud of the helical fluctuations revealing the quantum critical properties arises in a significant range of concentrations in the region of 0–5 K.

In conclusion we suggest a P - T phase diagram of an itinerant magnet with an extended helical fluctuation area, which may provide certain insight to the non-Fermi-liquid behavior and partial order of MnSi at high pressure and low temperature [17,18] (Fig. 13).

ACKNOWLEDGMENT

We gratefully acknowledge the technical support of A. A. Bykov, V. A. Sidorov, P. V. Zinin, and M. Costantino.

- [1] J. D. Thompson, Z. Fisk, and G. G. Lonzarich, *Physica B* **161**, 317 (1990).
- [2] C. Pfleiderer, G. J. McMullan, and G. G. Lonzarich, *Physica B* **206-207**, 847 (1995).
- [3] C. Thessieu, J. Flouquet, G. Lapertot, A. N. Stepanov, and D. Jaccard, *Solid State Commun.* **95**, 707 (1995).
- [4] C. Meingast, Q. Zhang, T. Wolf, F. Hardy, K. Grube, W. Knafo, P. Adelman, P. Schweiss, and H. v. Löhneysen, Resistivity of $Mn_{1-x}Fe_xSi$ Single Crystals Evidence for Quantum Critical Behavior, in *Properties and Applications of Thermoelectric Materials*, edited by V. Zlatić, and A. C. Hewson, NATO Science for Peace and Security Series B Physics and Biophysics (Springer, Dordrecht, 2009).
- [5] A. Bauer, A. Neubauer, C. Franz, W. Münzer, M. Garst, and C. Pfleiderer, *Phys. Rev. B* **82**, 064404 (2010).
- [6] A. E. Petrova, S. Yu. Gavrilkin, D. Menzel, and S. M. Stishov, *Phys. Rev. B* **100**, 094403 (2019).
- [7] A. E. Petrova, S. Y. Gavrilkin, G. V. Rybalchenko, D. Menzel, I. P. Zibrov, and S. M. Stishov, *Phys. Rev. B* **103**, L180401 (2021).
- [8] L. J. Bannenberg, R. M. Dalgliesh, T. Wolf, F. Weber, and C. Pappas, *Phys. Rev. B* **98**, 184431 (2018).
- [9] C. Pappas, A. O. Leonov, L. J. Bannenberg, P. Fouquet, T. Wolf, and F. Weber, *Phys. Rev. Res.* **3**, 013019 (2021).
- [10] S. V. Grigoriev, O. I. Utesov, N. M. Chubova, C. D. Dewhurst, D. Menzel, and S. V. Maleyev, *J. Exp. Theor. Phys.* **132**, 588 (2021).
- [11] C. Pappas, E. Lelièvre-Berna, P. Falus, P. M. Bentley, E. Moskvin, S. Grigoriev, P. Fouquet, and B. Farago, *Phys. Rev. Lett.* **102**, 197202 (2009).
- [12] S. V. Grigoriev, E. V. Moskvin, V. A. Dyadkin, D. Lamago, T. Wolf, H. Eckerlebe, and S. V. Maleyev, *Phys. Rev. B* **83**, 224411 (2011).
- [13] S. M. Stishov, A. E. Petrova, S. Khasanov, G. K. Panova, A. A. Shikov, J. C. Lashley, D. Wu, and T. A. Lograsso, *Phys. Rev. B* **76**, 052405 (2007).
- [14] M. Janoschek, M. Garst, A. Bauer, P. Krautscheid, R. Georgii, P. Böni, and C. Pfleiderer, *Phys. Rev. B* **87**, 134407 (2013).
- [15] A. M. Belemuk and S. M. Stishov, *Phys. Rev. B* **95**, 224433 (2017).
- [16] A. M. Belemuk and S. M. Stishov, *Phys. Rev. B* **104**, 064404 (2021).
- [17] C. Pfleiderer, S. R. Julian, and G. G. Lonzarich, *Nature (London)* **414**, 427 (2001).
- [18] C. Pfleiderer, D. Reznik, L. Pintschovius, H. v. Löhneysen, M. Garst, and A. Rosch, *Nature (London)* **427**, 227 (2004).